Advances in Water Resources 33 (2010) 361–371

Contents lists available at ScienceDirect

Advances in Water Resources

journal homepage: www.elsevier.com/locate/advwatres

Simulation of the subsurface mobility of carbon nanoparticles at the field scale

Erin Cullen [a], Denis M. O'Carroll [a,*], Ernest K. Yanful [a], Brent Sleep [b,1]

[a] Department of Civil and Environmental Engineering, University of Western Ontario, London, ON, Canada N6A 5B9
[b] Department of Civil Engineering, University of Toronto, 35 St. George St., Toronto, ON, Canada M5S 1A4

ARTICLE INFO

Article history:
Received 7 July 2009
Received in revised form 2 December 2009
Accepted 3 December 2009
Available online 11 December 2009

Keywords:
Nanoparticles
Mobility
Subsurface
Carbon nanotubes
nC_{60}

ABSTRACT

The production and use of nanomaterials will inevitably lead to their disposal in the natural environment. To assess the risk that these materials pose to human and ecosystem health an understanding of their mobility and ultimate fate is essential. To date, however, relatively little research has been conducted on the fate of nanoparticles in subsurface systems. In this study the subsurface mobility of two carbon nanoparticles: nano-fullerenes (nC_{60}) and multi-walled carbon nanotubes (MWCNTs) is assessed. A two-dimensional finite element model was used to simulate the movement of these nanoparticles under a range of hydrologic and geological conditions, including a heterogeneous permeability field. The numerical model is based on colloid filtration theory (CFT) with a maximum retention capacity term. For the conditions evaluated the carbon nanotubes are much more mobile than nC_{60} due to the smaller collector efficiency associated with carbon nanotubes. However, the mobility of nC_{60} increased significantly when a maximum retention capacity term was included in the model. Model results also demonstrate that, for the systems examined, nanoparticles were predicted to be less mobile in heterogeneous systems compared to the homogeneous systems with the same average hydraulic properties.

1. Introduction

Carbon based nanoparticles are being developed for a wide variety of commercial applications including biomedical technologies, cosmetics and electronics (e.g. [19,50,17,29]). With increased production and use, it is inevitable that nanoparticles will reach subsurface aquifers (e.g., due to release of industrial wastewaters, accidental spills or landfill leakage). The limited toxicity work completed to date has been inconclusive (e.g. [18,26,13,32,42,14,40,30]). For example, studies suggest that nC_{60} has anti-bacterial properties and could cause genotoxicity to human lymphocytes [8,26]. Carbon nanotubes (CNTs) are also a concern because their shape and size is similar to asbestos and could cause pulmonary diseases, including fibrosis and cancer [18,14,40]. In a study conducted in mice lungs, Lam et al. [18] found that single-walled carbon nanotubes (SWCNT) were more toxic than quartz, which is currently considered a serious occupational health and safety hazard. Due to health and ecosystem impact concerns an understanding of nanoparticle mobility in the environment is imperative. The mobility of carbon based nanoparticles is an important factor in determining the risk associated with their release to the environment.

Experimental studies have evaluated the mobility of multi-walled carbon nanotubes (MWCNTs), SWCNTs and nC_{60} aggregates and found that mobility varied greatly [19,20,6,11,23,49,24]. Although results from mobility studies are difficult to compare as experimental conditions are frequently different (e.g., grain size distribution, pore water velocity, nanoparticle preparation methods) comparison of results does help elucidate general trends in mobility. The studies of Lecoanet et al. are particularly useful because these authors tested the mobility of a range of nanoparticles under the same experimental conditions [19,20]. They reported that SWCNTs were more mobile than nC_{60} aggregates. Their study was conducted in glass bead packed columns at pore water velocities much higher than expected in the subsurface (i.e., minimum pore water velocity 80 m/d). Other studies investigating the mobility of nC_{60}, SWCNTs and MWCNTs in sand packed columns suggest that carbon nanotubes are mobile under conditions expected in the subsurface (e.g., pore water velocity) [6,11,23,24]. Previous studies generally report greater nC_{60} and MWCNT mobility with increasing pore water velocity [6,23,24]. Jaisi et al. [11] also found that aqueous phase chemistry had significant impacts on SWCNT mobility and postulated that straining may be an important SWCNT retention mechanism in porous media. For nC_{60}, however, Li et al. [23] suggested that straining was not an important retention mechanism and reported decreased mobility with decreasing porous media grain size. These limited experimental studies suggest that carbon nanoparticles are mobile in relatively short column experiments (i.e., 10 cm column length) however further work is necessary to determine if they will travel significant distances in the field.

* Corresponding author.
E-mail address: docarroll@eng.uwo.ca (D.M. O'Carroll).
[1] Fax: +1 416 978 3674.

0309-1708/$ - see front matter © 2010 Elsevier Ltd. All rights reserved.
doi:10.1016/j.advwatres.2009.12.001

Although laboratory studies have investigated nanoparticle mobility, very few numerical models have been developed to specifically simulate carbon based nanoparticle mobility. Li et al. [23] developed a one-dimensional numerical simulator, based on colloid filtration theory (CFT) with the addition of a site blocking term, to simulate nC_{60} transport in homogeneous porous media column experiments. They found that the numerical simulator, with the inclusion of the site blocking term, was able to provide good agreement between experimental observations and model results. Liu et al. [24] found similar results when they modeled observed MWCNT breakthrough curves. In both of these studies reasonable agreement between model and experimental results was achieved without the inclusion of straining in the numerical model.

Numerical models have not been used to investigate the mobility of carbon based nanoparticles at the field scale. However, numerical models have been used to investigate colloid transport in larger two- and three-dimensional systems (e.g. [34,41,4,25,27,2,3,28,36]). These studies suggest that field scale heterogeneities are important in determining the mobility of viruses and colloids in the subsurface. For example, Sun et al. [41] and Bhattacharjee et al. [4] both used random and layered physical and geochemical heterogeneities to assess colloid and virus transport in porous media. These studies found that colloid size, degree of heterogeneity (e.g., physical and geochemical) and attachment efficiency significantly impacted colloid mobility. The domain size in these two studies was relatively small (1 m × 3 m), the grain size did not vary with permeability (i.e., uniform grain size) and only one hydraulic gradient was investigated (0.01). Other studies have investigated the transport of colloids at the field scale in more complex 3D numerical simulations and found that coupling the colloid removal rate to spatially varying aquifer permeability improved modeling results (e.g. [34,27,28,36]). These studies, however, assumed an infinite number of sites for colloid retention on the soil surface. Coupled experimental and numerical model studies suggest that this may not be the case for carbon based nanoparticles [23,24].

Much of the work completed to date has evaluated the mobility of nanoparticles in one-dimensional glass bead or sand column experiments under conditions that are not representative of those that would be found in subsurface environments (e.g., large pore water velocity, no heterogeneities) [19,20,11,23,24]. Further work is therefore necessary to explore the mobility and associated risk of carbon based nanoparticles at the field scale. The objective of this study is to explore the mobility of carbon based nanoparticles at the field scale using a numerical simulator. Nanoparticle mobility is explored in heterogeneous domains under conditions representative of those encountered in the subsurface. This work utilizes a sensitivity analysis approach to determine the importance of hydrologic and transport parameters on carbon based nanoparticle mobility.

2. Model development

The transport of carbon based nanoparticles in saturated porous media can be described using mass balance equations of nanoparticles in the aqueous phase and those associated with the solid-phase [23]:

$$\frac{\partial C}{\partial t}+\frac{\rho_b}{n}\frac{\partial S}{\partial t}-\nabla\cdot(\overline{D}\cdot\nabla C)+\bar{v}\cdot\nabla C=0 \tag{1}$$

$$\frac{\rho_b}{n}\frac{\partial S}{\partial t}-K_{att}\psi_{att}C=0 \tag{2}$$

where C is the concentration of nanoparticles in the aqueous phase [M/L^3], S is the concentration of attached (or solid-phase) nanoparticles [M/M], t is the time [T], ρ_b is the soil bulk density [M/L^3] and n is the porosity [–]. $\overline{D}$ is the hydrodynamic dispersion tensor [L^2/T] and $\bar{v}$ is the pore water velocity vector [L/T]. K_{att} is the nanoparticle attachment rate [1/T] and ψ_{att} is a blocking function [–].

In this system of equations straining and detachment from the solid surface have been neglected, consistent with experimental observations of MWCNT and nC_{60} transport [23,24]. Jaisi et al. [11] suggest that straining could be an important removal mechanism when SWCNTs agglomerate and are transported through the porous media in bundles. The study of Liu et al. [24] reported very limited agglomeration for MWCNTs, therefore MWCNT straining due to agglomeration has been neglected in this study. The degree of bundling and rate of particle aggregation, however, will vary depending on the preparation method of the carbon nanotubes in aqueous solutions as well as the aqueous phase chemistry [35,39]. Detachment has not only been neglected in previous modeling studies of MWCNT and nC_{60} transport, but also in many previous colloid transport studies that found it had limited impact on predicted aqueous phase concentrations under typical subsurface conditions (e.g. [44,45,47,48,5,43]). Therefore, removal of the nanoparticles from the aqueous phase is assumed to be due to mechanisms traditionally associated with colloid filtration theory (e.g., deposition, interception and sedimentation) [46,23,24] where:

$$K_{att}=\frac{3}{2}\left(\frac{1-n}{d_{50}}\right)\alpha\eta_o v \tag{3}$$

where d_{50} is the median grain size [L], η_o is the single collector removal efficiency [–] and α is the collision efficiency factor [–]. Traditional colloid filtration theory does not include a site blocking term. However, it has been proposed that this mechanism is important in the transport of nanoparticles through porous media [23,24]. In these studies it was observed that nanoparticle transport could not be predicted using traditional colloid filtration due to delayed nanoparticle breakthrough in column experiments. These authors suggested that the sand collector surface had a finite retention capacity, consistent with previous studies of colloid transport (e.g. [12]). With time the retention capacity of the collector surfaces would be achieved and nanoparticles would no longer be removed by these collectors. As such the retention rate of the nanoparticles would initially be large and decrease with time, leading to delayed nanoparticle breakthrough. Site blocking has been incorporated into the conceptual model, consistent with reported studies:

$$\psi_{att}=\left(1-\frac{S}{S_{\max}}\right) \tag{4}$$

where $S_{\max}$ is the particle retention capacity [M/M]. Initially there are no nanoparticles associated with the solid phase (i.e., $S=0$; pristine aquifer conditions) and the site blocking term is unity. With increased nanoparticle attachment, S approaches $S_{\max}$ and the site blocking term approaches 0. A relation for $S_{\max}$ was proposed by Li et al. [23] for nC_{60} particles:

$$S_{\max}=19.6\left[\left(\frac{v d_c}{D_m}\right)^{1/3}\left(\frac{d_c}{d_M}\right)\right]^{-1.2} \tag{5}$$

Here D_m is the molecular diffusion coefficient [L^2/T] calculated from the Stokes–Einstein equation, d_c is the mean diameter of the collector [L] and d_M is the mean diameter of medium sand (0.5 mm). d_M is essentially an empirical constant that was used in the development of Li et al. [23] to obtain a dimensionless form of the diffusive flux across a boundary layer surrounding a collector. This relation for $S_{\max}$ is based on hydrodynamic parameters as suggested in previous studies (e.g. [15,16]). Li et al. [23] found that the inclusion of this relationship provided a good fit of $S_{\max}$ to the normalized mass flux in their study. A similar relationship has not been developed for carbon nanotubes, as a result a constant $S_{\max}$, consistent with the range

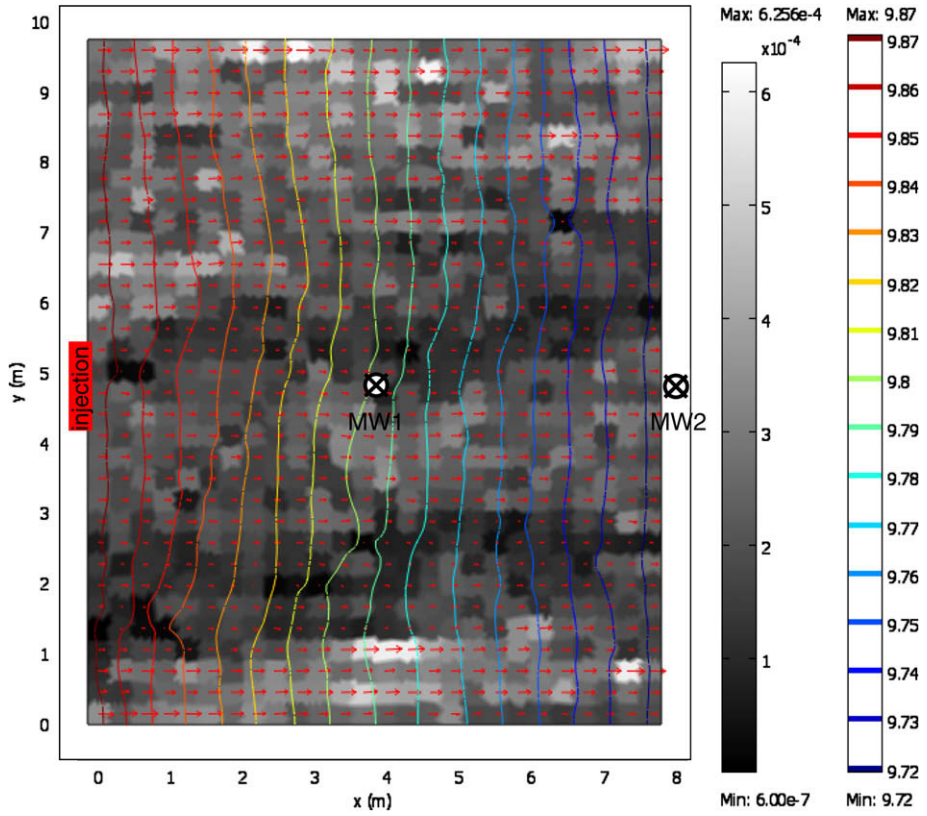

Fig. 1. Representative domain showing K [m/s] (blocks), H [m] (contour lines) and v [m/s] (arrows). The injection location is shown on the left side. Monitoring wells MW1 and MW2 are shown as labelled.

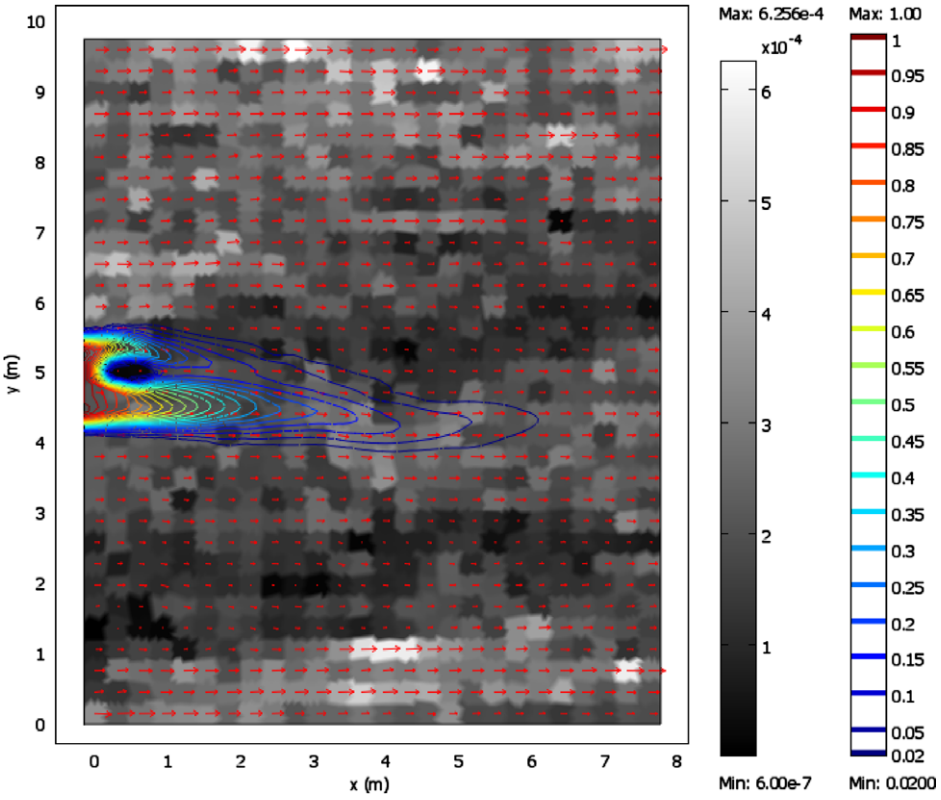

Fig. 2. Concentration of aqueous phase nC_{60} in a representative heterogeneous domain after 4 d of injection.

Table 1
Model simulations and parameters.

Case	Name	Carbon nanoparticle	C_o [mg/L]	dH/dL [–]	α_L [m]	α_T [m]	n [–]	α [–]	S_{max} [mg/g]
1	Heterogeneous vs homogeneous	nC_{60} MWCNT	1	0.02	0.3	0.0075	0.36	0.0002	n/a
2	Blocking	nC_{60}	1	0.02	0.3	0.0075	0.36	0.0002	0.002–0.033
3	Blocking & collision efficiency	MWCNT	1	0.02	0.3	0.0075	0.36	0.0002 0.002 0.02 0.2	1.18×10^{-3}
4	Longitudinal dispersivity	nC_{60} MWCNT	1	0.02	0.6 0.3 0.15 0.075	0.0075	0.36	0.0002	n/a
5	Transverse dispersivity	nC_{60} MWCNT	1	0.02	0.3	0.0075 0.025 0.03 0.06	0.36	0.0002	n/a
6	Transverse dispersivity & blocking	MWCNT	1	0.02	0.3	0.0075 0.06	0.36	0.0002	1.18×10^{-5}
7	Hydraulic gradient	nC_{60} MWCNT	1	0.002 0.011 0.02 0.11 0.20	0.3	0.0075	0.36	0.0002	n/a

of values reported by Li et al. [23] or Liu et al. [24], is used in this study.

The single collector contact efficiency, η_o, is often assumed to be the sum of three independent transport mechanisms: gravity, diffusion and interception as described by [51]:

$$\eta_o = \eta_G + \eta_D + \eta_I \tag{6}$$

For the nC_{60} particles, η_o was calculated according to the Tufenkji and Elimelech [46] method for spherical particles. However, because of the large aspect ratio of CNTs, a new relation for η_o was employed for MWCNT following Liu et al. [24].

COMSOL Multiphysics version 3.4a (Burlington, MA, USA) was used to simulate flow and nanoparticle transport in this study. This software uses the finite element method to solve systems of partial differential equations. An implicit time-stepping scheme was selected for a time-dependent analysis. The COMSOL model has also been validated by comparing model results to experimental data [24] and a finite difference compositional simulator [38].

In this study the mobility of carbon based nanoparticles is investigated using aquifer statistics derived from a field site in Oscoda, MI [21,22,31,33,1,7]. The field site is comprised of relatively homogeneous glacial outwash sands 8 m in depth and is underlain by a thick clay layer. This site was subject to extensive characterization as part of a surfactant enhanced aquifer remediation field trial. Twelve vertical and directional cores were obtained and divided into 167 subsamples for further grain size distribution and hydraulic conductivity analysis. This information was then used to develop 16 non-uniform permeability fields using conditional sequential Gaussian simulation (SGS) [21,22,33,1,7]. With the exception of the homogeneous case simulation, the mobility of the carbon based nanoparticles was assessed using all 16 permeability fields for all cases presented. The mean hydraulic conductivity is 16.8 m/d and the variance of the lognormal transformed K field is 0.29 [22]. Although the aquifer was considered to be relatively homogeneous, measured hydraulic conductivities varied between 1 and 48 m/d [21,22,31,7].

Consistent with the field site, the model domain used in this study was 7.925 m × 9.754 m in the horizontal and vertical directions, respectively. The domain was divided into 26 vertical columns and 32 horizontal rows ($dx = dy = 30.48$ cm). The resulting grid blocks are assumed to have constant K and d_{50} values (Fig. 1). In all cases the aquifer is assumed to be completely saturated. The model domain was further divided into a finite element mesh of 3188 Lagrangian quadratic triangular elements which contained 19,461 degrees of freedom. Each element was approximately 0.02 m^2 in area. Further refinement in the element mesh resulted in no significant change in the model solution.

The flow regime was determined for each of the 16 permeability fields and hydraulic gradients, assuming steady-state flow conditions. The vertical to horizontal permeability ratio was assumed to be 0.5 to account for anisotropy [7]. The top and bottom domain boundaries were subject to Type II (Neumann) no flow boundary conditions and the right and left side boundaries were subject to Type I (Dirichlet) constant head boundary conditions. In this study the sensitivity of model results to model parameters was assessed. The range of model parameters considered is found in Table 1.

Nanoparticle mass balance equations were solved by assuming no nanoparticle flux across the top and bottom boundaries. A Dirichlet boundary condition was used to inject nanoparticles at the upstream side of the domain and the following boundary condition was used at the downstream boundary:

$$D \cdot \nabla C - vC = \frac{K_{xx}}{n}\frac{dH}{dx}C \tag{7}$$

where K_{xx} is the horizontal component of the hydraulic conductivity [L/T] and H is water head [L]. The Dirichlet boundary condition

Table 2
Carbon nanoparticle properties.

	d_p (m)	l (m)	ρ_p (g/cm^3)	A [J]
MWCNT[a]	4.5×10^{-8}	5.0×10^{-6}	2.60	–
nC_{60}	1.05×10^{-7}[b]	–	1.41[c]	4.71×10^{-21}[d]

Note that Hamaker constant (A) are not reported for MWCNTs as they are not required in the calculation of η_o.

[a] [24].
[b] In the range of aggregate diameters reported in the literature [6,5,23].
[c] [6].
[d] [23].

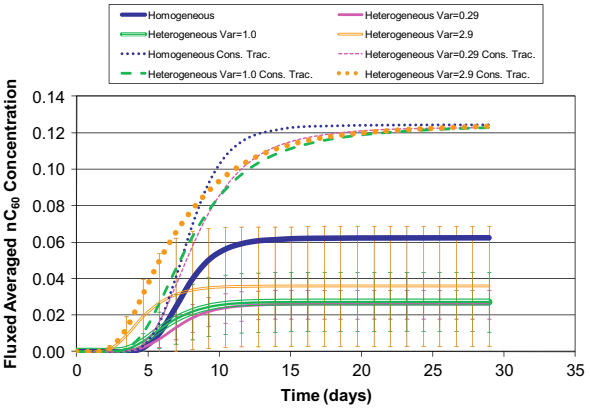

Fig. 3. Flux averaged nC_{60} concentrations for the heterogeneous (average of 16 realizations) cases with different permeability variance and homogeneous domains at the downstream domain boundary. Error bars indicate one standard deviation about the mean.

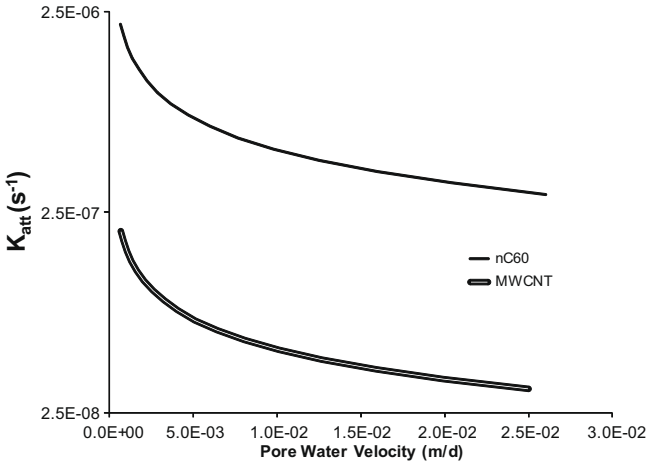

Fig. 5. Nanoparticle attachment rate as a function of pore water velocity. It is assumed that the hydraulic gradient is 0.002 and the collision efficiency is 0.0002.

simulates the release of nanoparticles over a 1.2 m screen interval on the left model boundary (Fig. 1):

$$C(0,y,t) = \begin{cases} 0, & y < 4.3 \text{ m} \\ C_o, & 4.3 < y < 5.5 \text{ m} \quad \text{for } t > 0 \\ 0, & y > 5.5 \text{ m} \end{cases} \tag{8}$$

Additional monitoring wells (sampling point locations) are simulated at the center of the domain and at the center of the downstream boundary (MW1 and MW2 in Fig. 1).

The mobility of the representative carbon based nanoparticles at the field scale was assessed in this study (MWCNT and nC_{60}). These nanoparticles were selected because of their anticipated widespread use, concern related to their fate in the environment (e.g. [29]) and the availability of model input parameters. The properties of the nanoparticles are summarized in Table 2.

3. Results and discussion

The mobility of the representative carbon based nanoparticles at the field scale is assessed under a range of hydrologic and geological conditions that would be expected in the field (e.g., hydraulic gradient, dispersivity). The different cases assessed along with the range of values for each parameter in the sensitivity analysis are presented in Table 1.

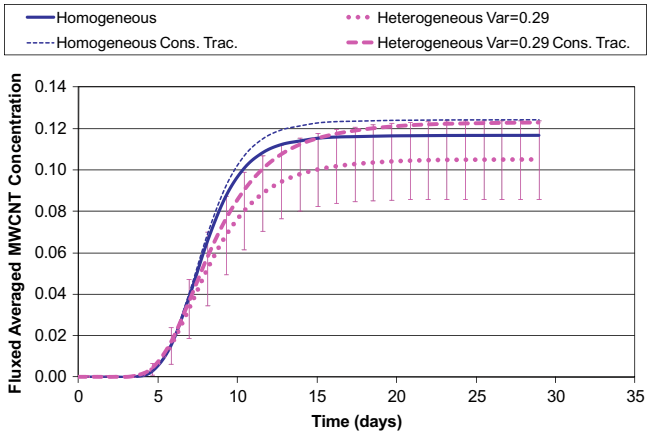

Fig. 4. Normalized MWCNT concentrations for the heterogeneous (average of 16 realizations) and homogeneous domains at the downstream domain boundary. Error bars indicate one standard deviation about the mean.

3.1. Effect of heterogeneity on transport

To explore the impact of field scale heterogeneities on carbon based nanoparticle mobility, a suite of transport simulations was conducted for the two carbon based nanoparticles in the 16 heterogeneous domains (Case 1, Table 1). An additional suite of simulations was conducted in a homogeneous domain with a uniform hydraulic conductivity of 16.8 m/d (the mean of the natural logarithm of K [21]) for comparison purposes. In this suite of simulations particle site blocking is neglected ($\psi_{att} = 1$). In the heterogeneous domains, the carbon based nanoparticles encounter regions of high and low pore water velocities as well as different attachment rates due to different velocities and soil grain sizes, significantly altering the transport characteristics (see Fig. 2 for nC_{60}, MWCNT results not shown). In these domains nanoparticle transport is much less uniform in comparison to a homogeneous domain, with preferential nanoparticle transport through the more permeable zones. The impact of heterogeneity is also evident in the conservative tracer breakthrough curve which shows more dispersion than the homogeneous case (Fig. 3). Most significantly, the carbon based nanoparticles reached a higher flux averaged effluent concentration in the homogeneous domain in comparison to the representative heterogeneous domains (Fig. 3 for nC_{60}, and Fig. 4 for MWCNT). The peak nC_{60} concentrations in the homogeneous domain were outside of the 95% confidence interval about the mean of the heterogeneous cases and the peak MWCNT concentrations for the homogeneous domain were above the mean peak heterogeneous results, but not outside of the 95% confidence interval about the mean of the heterogeneous cases. These differences can be attributed to spatially variable grain (collector) size, subsequent spatially variable pore water velocities and attachment rates, K_{att}, which are a function of pore water velocity in the heterogeneous domain (i.e., η_o is a function of pore water velocity). As pore water velocity decreases, η_o increases, resulting in more attachment of nanoparticles at the collector surface thereby decreasing nanoparticle mobility. The relationship between grain size, pore water velocity and K_{att} is highly nonlinear with the attachment rates significantly increasing with decreasing grain size and pore water velocity (Fig. 5). The significant difference between the heterogeneous and homogeneous nC_{60} effluent concentrations highlights the importance of pore water velocity on the collector efficiency. The transport of nC_{60} into lower permeability regions, where the lower pore velocity and smaller grain size both contribute to greater attachment rates, leads to significantly more retention of nC_{60} than in the homogeneous domain with uniform velocity and grain

size. In contrast, the effect of heterogeneity on conservative tracer transport is much less significant. These model predictions show that the assumption of homogeneous subsurface conditions overestimates nanoparticle mobility by neglecting the increased retention in low permeability zones.

The MWCNT and nC_{60} nanoparticles reach the downstream boundary at approximately the same time (e.g., MWCNTs achieve 5% of the effluent plateau concentration in 4.8 d and the nC_{60} in 4.1 d), however, the maximum flux averaged concentration are distinctly different. For example, the average steady-state flux averaged concentrations are 0.105 and 0.026 mg/L for MWCNTs and nC_{60}, in the heterogeneous domain. This difference in mobility can be attributed to two factors: nanoparticle shape and size. The MWCNTs are long cylinders (5000 nm) with a small diameter (45 nm), whereas nC_{60} aggregates are spherical with a diameter of 105 nm. Both nanoparticle shape and size are incorporated into the numerical simulator through the theoretical collector efficiency term (η_o). For the two nanoparticles the diffusion term dominates the theoretical collector efficiency. In the heterogeneous domain the MWCNT theoretical collector efficiency (η_o) (0.006–1.18) is much smaller than that for nC_{60} (0.074–86.7). This is expected as MWCNTs are the larger nanoparticle, decreasing the importance of Brownian diffusion. η_D is also a function of pore water velocity and the soil grain size, which were the same for both nanoparticles in this case.

Interestingly, the difference between the steady-state flux averaged concentration for the heterogeneous and homogeneous cases for the MWCNTs (0.018 mg/L) is not as large as the difference in the nC_{60} case (0.037 mg/L). This implies that, for the range of pore water velocities and soil grain sizes in these simulations, pore water velocity and soil grain size have a larger impact on nC_{60} transport than they do on the MWCNTs, consistent with the larger range of theoretical collector efficiencies for nC_{60}. These simulations neglect site blocking (ψ_{att} in Eq. (2)) which would impact these results. In addition, it was assumed that the collision efficiency for each nanoparticle is the same. This may not be the case as different nanoparticles will have different surface characteristics, which will impact the collision efficiency.

An additional suite of simulations were conducted to explore the impact of the degree of heterogeneity on nC_{60} transport. The variance of the lognormal transformed K field ($\sigma^2 \ln K$) was increased to 1.0 and 2.9. Increasing the variance to 2.9 resulted in an earlier appearance of nC_{60} at the downstream boundary in comparison to the lower variance cases and the homogeneous case (Fig. 3). For example, the time at which the flux averaged effluent concentration achieves 5% of the maximum flux averaged effluent concentration increases from 2.38 d, at a variance of 2.9, to 3.56, 4.13 and 4.79 d when the system is changed to variances of 1.0, 0.29 and the homogeneous case, respectively. In addition the average maximum flux averaged effluent concentrations are greater for the higher variance case suggesting the nC_{60} flow through higher permeability flow paths with lower attachment rates. It should be noted that the 95% confidence intervals about the mean for the heterogeneous cases overlap and that the confidence intervals increase with increased variance. In all cases the flux averaged effluent concentrations for the homogeneous domain were larger than the heterogeneous domains for all variances examined.

Regulatory limits of allowable MWCNT or nC_{60} concentrations in groundwater have not yet been determined; therefore, it is not obvious if regulator concern should be greater for MWCNTs, which are more mobile in this case, in comparison to nC_{60} as maximum allowable exposure concentrations for nC_{60} may be much lower than MWCNTs.

3.1.1. Effect of blocking on nC_{60} deposition

Previous one-dimensional column studies suggest a limited retention capacity of porous media for carbon based nanoparticles [23,24]. In Case 1 an infinite retention capacity was assumed, consistent with many published studies for colloid transport (e.g. [4,2,3]). In this suite of simulations (Case 2, Table 1) the impact of a finite retention capacity, and subsequent site blocking, on the mobility of nC_{60} aggregates was investigated. A large value of S_{max} yields a site blocking function very close to 1 (clean bed/pristine conditions), essentially ensuring that the adsorbed mass (S) of nanoparticles will never reach S_{max} and therefore no nanoparticle site blocking will occur. With a lower S_{max} the adsorbed mass approaches S_{max} and the capacity of the solid phase to retain additional nanoparticles approaches zero. In this suite of simulations the value of S_{max} varied across the heterogeneous domain (0.0024–0.033 mg/g) as it is a function of pore water velocity and soil grain size (Eq. (5)), as proposed by Li et al. [23].

The inclusion of a blocking term significantly increases the maximum nC_{60} aqueous phase concentration at MW1 (Fig. 6). In the homogeneous domain normalized effluent concentrations are similar for approximately the first 10 d. After 10 d the site blocking term starts to become important as the retention capacity of the soil surface is approached, limiting availability of retention sites on the soil surface for additional nC_{60}. At this point normalized concentrations at MW1 start to diverge. In the heterogeneous domains, simulation results with and without site blocking are also

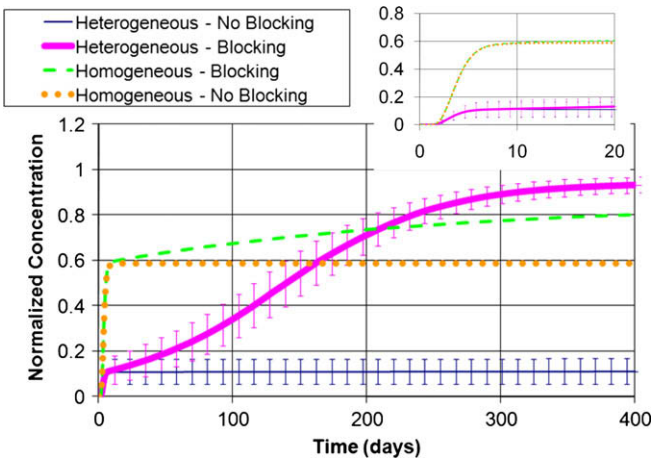

Fig. 6. Normalized nC_{60} concentration breakthrough curves for homogeneous and heterogeneous (average of 16 realizations) domains at MW1 including and not including a blocking function. Error bars indicate a 95% confidence interval about the mean. Inset shows the early time breakthrough.

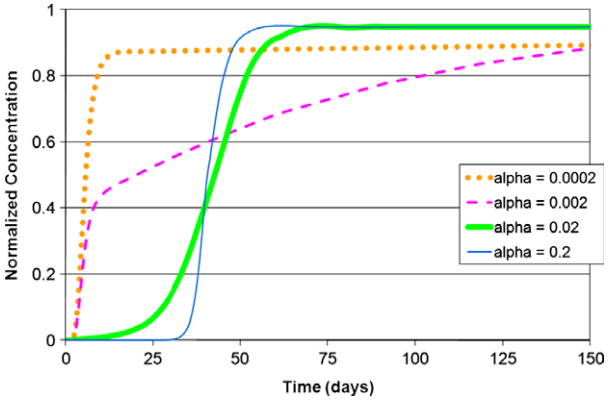

Fig. 7. Normalized concentration of MWCNT showing the combined effect of a constant S_{max} value and changing α values. $S_{max} = 1.18 \times 10^{-3}$ mg/g. Data shown is taken from MW1.

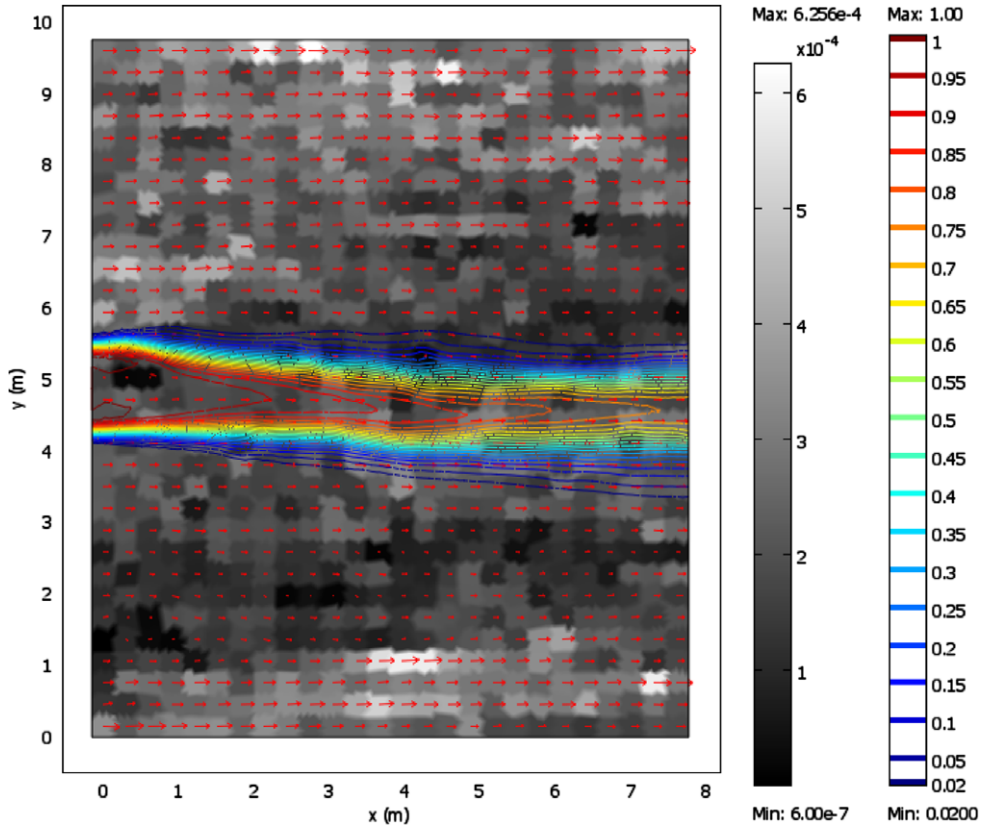

Fig. 8. Representative normalized aqueous phase MWCNT concentration after 40 d for a constant $S_{max} = 1.18 \times 10^{-3}$ mg/g and $\alpha = 0.0002$.

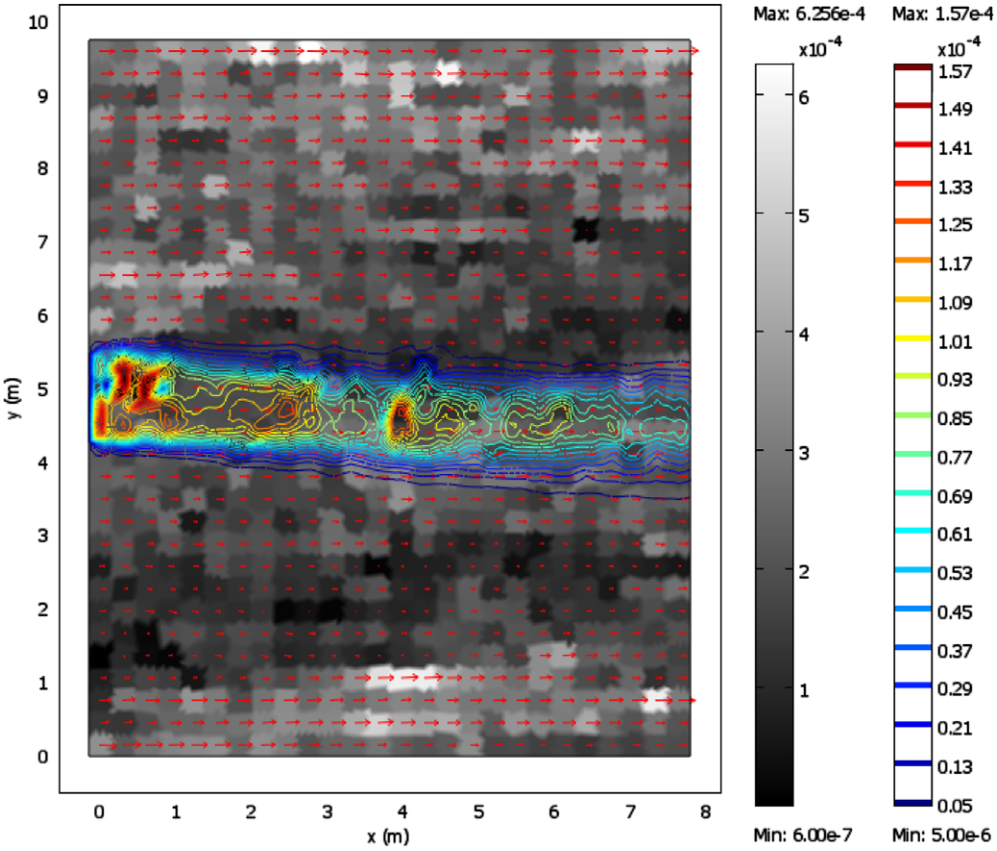

Fig. 9. Representative concentration of attached phase MWCNT after 40 d for constant $S_{max} = 1.18 \times 10^{-3}$ mg/g and $\alpha = 0.0002$.

initially similar (<10 d). However, the breakthrough curves are distinctly different at later times. At 400 d the average normalized effluent concentration in the heterogeneous domain is 10% when site blocking is ignored and 90% when site blocking is incorporated in the simulations. Note that the normalized effluent concentration is increasing at 400 d for the case when site blocking is incorporated since not all attachment sites have reached their maximum retention capacity. This demonstrates that model estimates that do not account for site blocking may significantly underestimate nanoparticle concentrations at receptor locations.

3.1.2. Combined effect of collision efficiency and maximum retention capacity

For the previous suite of simulations it was assumed that the collision efficiency was 0.0002, however this model parameter can vary by orders of magnitude (e.g. [4,19,46,23]). The collision efficiency is a function of aqueous phase chemistry as well as nanoparticle and collector surface charges. These surface charges are very sensitive to adsorbed polymers and coatings (e.g. [6,9,10]). An additional suite of simulations was carried out to explore the impact of the collision efficiency on MWCNT transport (Case 3, Table 1). For this suite of simulations a constant maximum retention capacity in the same range as that observed by Li et al. [23], was selected ($S_{max} = 1.18 \times 10^{-3}$ mg/g).

Increasing the collision efficiency from 0.0002 to 0.2 increases the time to achieve 5% of the maximum normalized MWCNT effluent concentration at MW1 since a greater proportion of nanoparticles striking the collector attach to it (Fig. 7). The combined effects of the attachment rate term (K_{att}) and the site blocking term (ψ_{att}) yielded interesting results. For example, the simulation with the largest collision efficiency (0.2) reached 95% of its maximum normalized concentration at MW1 faster than the next largest collision efficiency factor (0.02). The collision efficiency impacts the rate at which nanoparticles are attached to the solid phase and the site blocking term is related to the number of available attachment sites. As more mass is removed from the aqueous phase the nanoparticle mass associated with the solid phase, S, approaches S_{max} and ψ_{att} approaches zero. As ψ_{att} approaches zero the rate of nanoparticle removal from the aqueous phase also approaches zero. When the collision efficiency is large the rate of nanoparticle removal from the aqueous phase is initially large and the maximum retention capacity of the solid phase is achieved relatively quickly. In comparison, when the collision efficiency factor decreases to 0.02, the rate at which the maximum retention capacity is achieved is lower, resulting in a less sharp normalized MWCNT concentration at MW1.

At the lowest collision efficiency (0.0002) MWCNT breakthrough is rapid as only a small number of MWCNTs attach to the solid surface and are removed from the aqueous phase. In this case the MWCNT aqueous phase concentration is relatively high (Fig. 8) and the mass associated with the solid phase is relatively small (Figs. 9 and 10). In these heterogeneous domain simulations the MWCNTs flow through a range of hydraulic conductivities. In the less permeable zones the pore water velocity is smaller, as is the soil grain size, resulting in increased collector efficiencies. As a result the MWCNT mass associated with the solid phase is larger in the lower permeability zone. However, given the low collision efficiency, a significant amount of time is required to achieve the retention capacity (Fig. 10). In comparison, when the collision efficiency is large (0.2) the MWCNT concentration in the aqueous phase is comparatively smaller and more of the MWCNT mass is associated with the solid phase of all grain sizes since a large proportion of collisions between MWCNTs in the aqueous phase and the collector result in MWCNT attachment to the solid phase (Fig. 11). At the higher collector efficiency, the attached phase nanoparticle concentration is at the maximum retention capacity

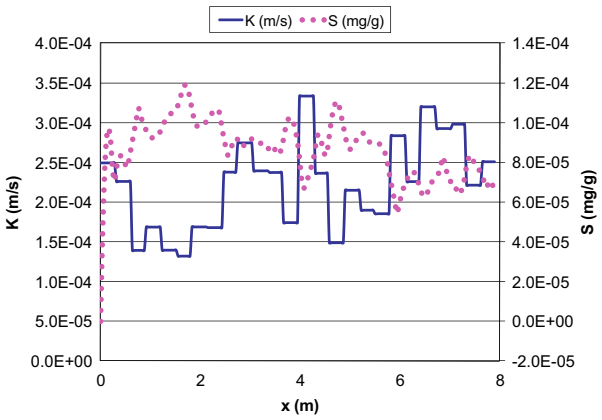

Fig. 10. Representative cross-section through the centre of the domain showing attached phase nanoparticles and hydraulic conductivity when collision efficiency is 0.0002.

(1.18×10^{-3} mg/g) in the first 5 m of the domain and drops off sharply in the remaining 3 m due to the high retention of MWCNTs in the first 5 m (Fig. 11).

The case when the collision efficiency is 0.002 is also interesting. In this case, the time at which 5% of the maximum normalized MWCNT concentration at MW1 is achieved is similar to the case of lower collision efficiency (0.0002). However, the breakthrough curves diverge at a normalized effluent concentration of 0.3. Lower MWCNT removal rates are achieved in the more permeable zones, whereas in the less permeable zones more MWCNTs are retained, as discussed above. As a result at early times a lower proportion of the MWCNTs are removed from the aqueous phase in the more permeable zones and most of the MWCNT removal occurs in the less permeable zones. With time, the attachment sites in the lower permeability zones reach their maximum retention capacity resulting in the slow rise in effluent concentrations (Fig. 7). For the case with a collision efficiency of 0.002 a larger proportion of collisions between the MWCNTs and the soil surface are successful, resulting in greater MWCNT retention. As a result these soils reach their retention capacity more quickly than the case of a collision efficiency of 0.0002.

At the end of the simulation the maximum normalized effluent concentration when $\alpha = 0.2$ is 98.5%, 3% higher than the simulation with the lowest collision efficiency factor. In both cases the solid phase has not reached its maximum retention capacity at the end of the simulation. These simulations suggest a complex relationship between the collision efficiency, collector efficiency, the soil maximum retention capacity and soil heterogeneity.

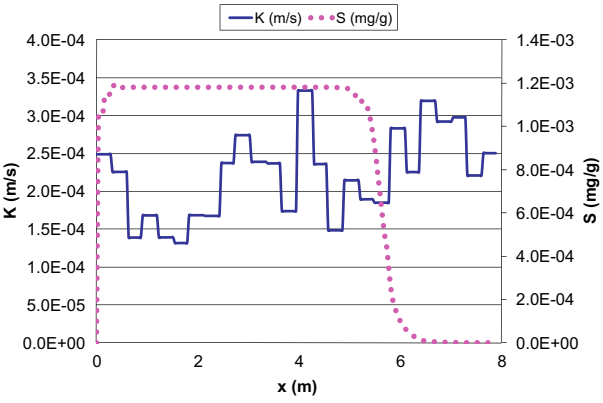

Fig. 11. Representative cross-section through the centre of the domain showing attached phase nanoparticles and hydraulic conductivity when collision efficiency is 0.2.

3.1.3. Effect of dispersivity on nanoparticle breakthrough

The magnitude of longitudinal and transverse dispersivity in the subsurface can vary widely and is often a function of the scale of characterization of the study site. Values as low as 0.0001 m and as high as 5500 m have been reported for longitudinal dispersivity [37]. Lemke et al. [22] quantified a longitudinal dispersivity of 0.3 m at this field site based on 3D modeling of an alcohol tracer test at the site and explored model sensitivities to transverse dispersivities ranging from 0.0075 to 0.06 m. A suite of simulations using the 16 heterogeneous domains were conducted to assess the importance of dispersion on the transport of carbon based nanoparticles at the field scale (Cases 4 and 5, Table 1). Longitudinal dispersivity has a very limited impact on nanoparticle transport in the heterogeneous domains used here for the range investigated (0.6–0.075 m) (results not shown). For the domains presented in this study more accurate determination of other model parameters (e.g., collision efficiency and maximum retention capacity) would likely have a greater impact on the accuracy of nanoparticle mobility predictions.

A second suite of simulations was conducted to assess the impact of transverse dispersivity on carbon based nanoparticle mobility (Case 5, Table 1). Increasing the magnitude of the transverse dispersivity decreased the maximum normalized MWCNT effluent concentration at MW2 to 55% of the low dispersivity case (Fig. 12). This suggests that transverse dispersivity, in addition to heterogeneity, is also an important factor controlling nanoparticle mobility. However, if a fully screened well, such as a drinking water well, is screened along the entire effluent boundary the mass flux from the domain is similar in each simulation (area under curve on Fig. 13). As the degree of heterogeneity increases it is expected that the variation in mass flux would be greater because the nanoparticles would encounter a broader range of soil grain sizes with a wider range of attachment rates.

In the simulations exploring the sensitivity of carbon based nanoparticle transport to transverse dispersivity it was assumed that the collector retention capacity was infinite (no blocking). An additional suite of simulations was conducted under the same conditions and assuming a maximum retention capacity of 1.18×10^{-5} mg/g (Case 6, Table 1). This maximum retention capacity was fit to a series of MWCNT column experiments in quartz sand [24]. In this case the MWCNT mass entering a well that is screened the entire length of the right boundary decreased in comparison to the case when site blocking is ignored and also decreased with increasing transverse dispersivity when blocking is incorporated (Fig. 14). After 11 d, a total of 17.7 ± 4.7 mg MWCNT entered the well when the transverse dispersivity was 0.0075 m compared to a total of 15.4 ± 6.5 mg MWCNT when the transverse

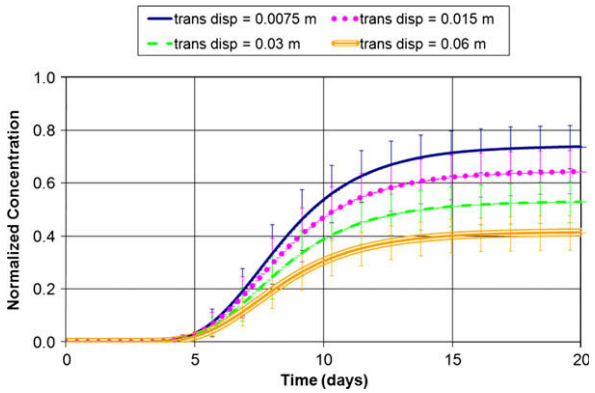

Fig. 12. Normalized MWCNT concentration breakthrough curves for constant longitudinal dispersivity and varying transverse dispersivity at MW2. Error bars indicate one standard deviation about the mean.

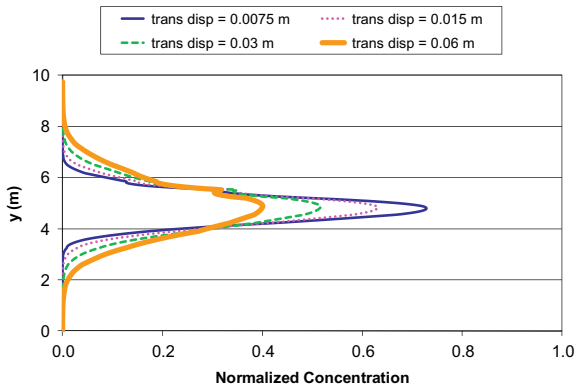

Fig. 13. Well screened along the entire depth of the right side of the domain showing MWCNT normalized aqueous phase concentrations after 1 year.

dispersivity was 0.06 m. Although the standard deviations do overlap, in all cases if results from the same domain are compared less mass exits the right boundary for the greater transverse dispersivity. With more spreading in the transverse direction, nanoparticles encounter collectors that have not reached their maximum retention capacity leading to more attachment in these zones. It is anticipated that this trend would continue with further increase in transverse dispersivity. However, with time the mass fluxes in all cases would be the same as the soils would reach their retention capacity.

3.1.4. Effect of velocity on nanoparticle breakthrough

The hydraulic gradient can vary considerably from site to site or even seasonally at the same site. At the field site used to generate the permeability realizations in this study the hydraulic gradient ranged between 0.002 and 0.13 [22]. To explore the impact of hydraulic gradient and pore water velocity on carbon based nanoparticle mobility the hydraulic gradient was varied between a very low gradient (0.002), which may be encountered in undisturbed conditions to a very high gradient (0.2) which may be encountered in disturbed conditions (i.e. in the vicinity of a pumping well) [21,22,7] (Case 7, Table 1).

The reduced hydraulic gradients decreased the maximum normalized effluent concentration (Figs. 15 and 16 for nC_{60} and MWCNT, respectively). The breakthrough curves are presented at MW1, which is the midpoint of the domain, however to normalize the breakthrough curves for the different hydraulic gradients the pore volume of the half the model domain was utilized in the calculation. In addition the two types of nanoparticles entered the domain across a 1.2 m interval of the 9.754 m upstream boundary further complicating normalization to pore volume. The maxi-

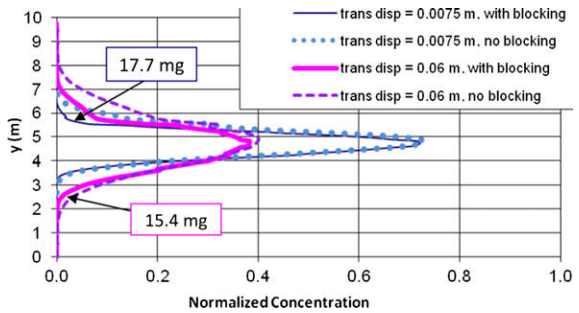

Fig. 14. Normalized aqueous phase concentration of MWCNT appearing in a well screened the full depth of the right side boundary after 11 d for two different values of transverse dispersivity with a S_{max} value of 1.18×10^{-5} mg/g and neglecting site blocking.

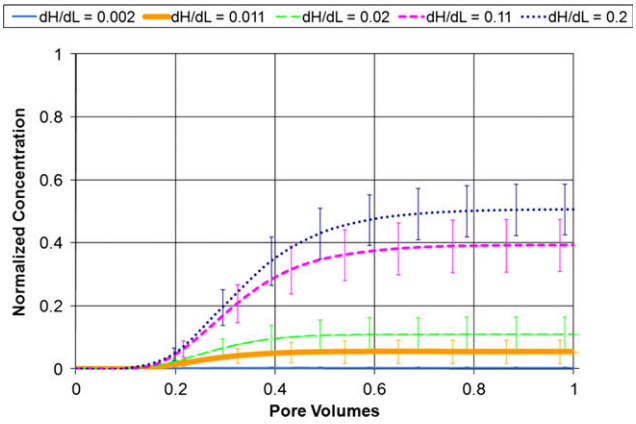

Fig. 15. Normalized nC_{60} concentration breakthrough curves for different hydraulic gradients at MW1. Error bars indicate a 95% confidence interval about the mean.

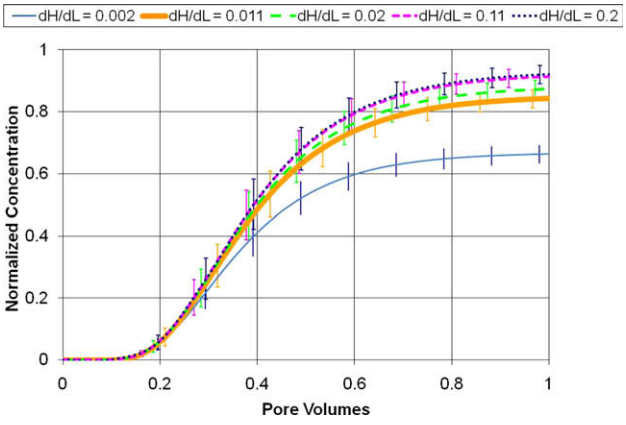

Fig. 16. Normalized MWCNT concentration breakthrough curves for different hydraulic gradients at MW1. Error bars indicate a 95% confidence interval about the mean.

mum effluent concentrations decrease with decreasing hydraulic gradient due to the reduced pore water velocity and subsequent increase in the K_{att} term (Fig. 5). For MWCNTs the maximum concentration at MW1 is 0.93 mg/L at a hydraulic gradient of 0.2 and decreases to 0.67 mg/L for a hydraulic gradient of 0.02. For nC_{60} the collector efficiency range increases from 0.014–17.5 at a hydraulic gradient of 0.2 to 0.380–442.1 at a hydraulic gradient of 0.002. Brownian diffusion is the largest contribution to the collector efficiency for the cases studied here. Also of note is that the reduction in maximum effluent concentration with decreasing velocity is greatest for the smallest nanoparticles studied (nC_{60}). This shows that pore water variations have a larger impact on the smaller nanoparticles as discussed above.

The groundwater velocity has a significant impact on carbon nanoparticle mobility with increased carbon nanoparticle mobility in scenarios where the groundwater velocity has been increased by human activities. This suggests that zones surrounding municipal water production wells are particularly susceptible given the larger hydraulic gradients and higher groundwater velocities in the vicinity of drinking water wells.

3.2. Summary and conclusions

The mobilities of two carbon nanoparticles (MWCNTs and nC_{60}) were assessed by modeling the release of each of these nanoparticles in both homogeneous and heterogeneous field sites. The maximum flux averaged concentrations of the nanoparticles at selected monitoring locations were lower for heterogeneous domains than for the equivalent homogeneous domains due to greater retention of nanoparticles in lower hydraulic conductivity zones where lower groundwater velocities and smaller soil grain sizes corresponded to higher attachment coefficients. Increasing the variance of the log hydraulic conductivity field by a factor of 10 decreased the first breakthrough times, due to preferential flow of the nanoparticles in the higher permeability soils, and also increased the maximum flux averaged concentrations but not to the level of the homogeneous domain predictions. The impact of heterogeneity on reducing maximum nanoparticle concentration relative to the homogeneous case was also greater for nC_{60} compared to MWCNTs, due to the higher collector efficiency associated with the nC_{60} size and shape relative to MWCNTs.

For the nanoparticles and soil conditions examined, nanoparticle transport was not sensitive to longitudinal dispersivity, but was sensitive to transverse dispersivity. The sensitivity to transverse dispersivity is attributed to the increased dispersive transport of nanoparticles into low hydraulic conductivity zones where groundwater velocities are low and collector efficiencies are correspondingly increased. Nanoparticle transport was also sensitive to overall hydraulic gradient and groundwater velocity, with larger hydraulic gradients and velocities resulting in less nanoparticle retention in soil and greater maximum concentrations at monitoring locations. This may be particularly significant in the vicinity of municipal water wells where high pumping rates will lead to high groundwater velocities and therefore higher concentrations of nanoparticles in the wells.

Nanoparticle transport and maximum concentrations are very sensitive to collision efficiency factors and blocking factors. At present, accurate methods to predict these factors a priori from soil and nanoparticle characteristics have not been developed. This is therefore an important area for future research. This study only investigated the mobility of two representative nanoparticles and showed that they could be mobile in subsurface systems. Given this mobility, appropriate measures should be taken to protect at-risk downstream receptors. It is anticipated that a wide variety of nanoparticles, beyond the two studied here, will ultimately be present in subsurface systems. Each of these nanoparticles will have different physical and chemical characteristics, significantly impacting their mobility. An assessment is therefore needed to quantify the risk these nanoparticles pose to ecosystem and human health. To do this detailed information related to nanoparticle mobility and toxicity will be necessary.

Acknowledgements

This research was supported by an Ontario Ministry of the Environment Best in Science Award.

References

[1] Abriola LM, Drummond CD, Hahn EJ, Hayes KF, Kibbey TCG, Lemke LD, et al. Pilot-scale demonstration of surfactant-enhanced PCE solubilization at the Bachman Road Site. 1. Site characterization and test design. Environ Sci Technol 2005;39(6):1778–90.
[2] Bekhit HM, Hassan AE. Two-dimensional modeling of contaminant transport in porous media in the presence of colloids. Adv Water Resour 2005;28:1320–35.
[3] Bekhit HM, Hassan AE. Stochastic modelling of colloid-contaminant transport in physically and geochemically heterogeneous porous media. Water Resour Res 2005;41:W02010. doi:02010.01029/02004WR003262.
[4] Bhattacharjee S, Ryan JN, Elimelech M. Virus transport in physically and geochemically heterogeneous subsurface porous media. J Contam Hydrol 2002;57:161–87.
[5] Chen KL, Elimelech M. Aggregation and deposition kinetics of fullerene (C-60) nanoparticles. Langmuir 2006;22(26):10994–1001.
[6] Cheng X, Kan AT, Tomson MB. Study of C60 transport in porous media and the effect of sorbed C60 on naphthalene transport. J Mater Res 2005;20:3244–54.

[7] Christ JA, Lemke LD, Abriola LM. Comparison of two-dimensional and three-dimensional simulations of dense nonaqueous phase liquids (DNAPLs): migration and entrapment in a nonuniform permeability field. Water Resour Res 2005;41:W01007. doi:01010.01029/02004WR003239.
[8] Dhawan A, Taurozzi JS, Pandey AK, Shan W, Miller SM, Hashsham SA, et al. Stable colloidal dispersions of C60 fullerenes in water: evidence for genotoxicity. Environ Sci Technol 2006;40(23):7394–401.
[9] Guzman KAD, Finnegan MP, Banfield JF. Influence of surface potential on aggregation and transport of titania nanoparticles. Environ Sci Technol 2006;40(24):7688–93.
[10] Hydutsky BW, Mack EJ, Beckerman BB, Skluzacek JM, Mallouk TE. Optimization of nano- and microiron transport through sand columns using polyelectrolyte mixtures. Environ Sci Technol 2007;41(18):6418–24.
[11] Jaisi DP, Saleh NB, Blake RE, Elimelech M. Transport of single-walled carbon nanotubes in porous media: filtration mechanisms and reversibility. Environ Sci Technol 2008;42(22):8317–23.
[12] Johnson PR, Elimelech M. Dynamics of colloid deposition in porous-media – blocking based on random sequential adsorption. Langmuir 1995;11(3): 801–12.
[13] Kang S, Pinault M, Pfefferle LD, Elimelech M. Single-walled carbon nanotubes exhibit strong antimicrobial activity. Langmuir 2007;23(17):8670–3.
[14] Klaine SJ, Alvarez PJJ, Batley GE, Fernandes TF, Handy RD, Lyon DY, et al. Nanomaterials in the environment: behaviour fate bioavailability and effects. Environ Toxicol Chem 2008;27(9):1825–51.
[15] Ko CH, Bhattacharjee S, Elimelech M. Coupled influence of colloidal and hydrodynamic interactions on the RSA dynamic blocking function for particle deposition onto packed spherical collectors. J Colloid Interf Sci 2000;229:554–67.
[16] Ko CH, Elimelech M. The shadow effect in colloid transport and deposition dynamics in granular porous media: measurements and mechanisms. Environ Sci Technol 2000;34(17):3681–9.
[17] Kostarelos K, Lacerda L, Pastorin G, Wu W, Wieckowski S, Luangsivilay J, et al. Cellular uptake of functionalized carbon nanotubes is independent of functional group and cell type. Nat Nanotechnol 2007;2(2):108–13.
[18] Lam C-W, James JT, McCluskey R, Hunter RL. Pulmonary toxicity of single-wall carbon nanotubes in mice 7 and 90 days after intratracheal instillation. Toxicol Sci 2004;77:126–34.
[19] Lecoanet HF, Bottero J-Y, Wiesner MR. Laboratory assessment of the mobility of nanomaterials in porous media. Environ Sci Technol 2004;38(19):5164–9.
[20] Lecoanet HF, Wiesner MR. Velocity effects on fullerene and oxide nanoparticle deposition in porous media. Environ Sci Technol 2004;38(16):4377–82.
[21] Lemke LD, Abriola LM. Dense nonaqueous phase liquid (DNAPL) source zone characterization: influence of hydraulic property correlation on predictions of DNAPL infiltration and entrapment. Water Resour Res 2004;40:W01511. doi:01510.01029/02003WR001980.
[22] Lemke LD, Abriola LM, Lang JR. Influence of hydraulic property correlation on predicted dense nonaqueous phase liquid source zone architecture, mass recovery and contaminant flux. Water Resour Res 2004;40:W12417. doi:12410.11029/12004WR003061.
[23] Li YS, Wang YG, Pennell KD, Abriola LM. Investigation of the transport and deposition of fullerene (C60) nanoparticles in quartz sands under varying flow conditions. Environ Sci Technol 2008;42(19):7174–80.
[24] Liu XY, O'Carroll DM, Petersen EJ, Huang QG, Anderson CL. Mobility of multiwalled carbon nanotubes in porous media. Environ Sci Technol 2009;43(21):8153–8.
[25] Loveland JP, Bhattacharjee S, Ryan JN, Elimelech M. Colloid transport in a geochemically heterogeneous porous medium: aquifer tank experiment and modeling. J Contam Hydrol 2003;65:161–82.
[26] Lyon DY, Adams LK, Falkner JC, Alvarez PJJ. Antibacterial activity of fullerene water suspensions: effects of preparation method and particle size. Environ Sci Technol 2006;40(14):4360–6.
[27] Maxwell RM, Welty C, Tompson AFB. Streamline-based simulation of virus transport resulting from long term artificial recharge in a heterogeneous aquifer. Adv Water Resour 2003;26(10):1075–96.
[28] Maxwell RM, Welty C, Harvey RW. Revisiting the cape cod bacteria injection experiment using a stochastic modeling approach. Environ Sci Technol 2007;41(15):5548–58.
[29] Mueller NC, Nowack B. Exposure modeling of engineered nanoparticles in the environment. Environ Sci Technol 2008;42(12):4447–53.
[30] Petersen EJ, Akkanen J, Kukkonen JVK, Weber Jr WJ. Biological uptake and depuration of carbon nanotubes by daphnia magna. Environ Sci Techol 2009;43(8):2969–75.
[31] Phelan TJ, Lemke LD, Bradford SA, O'Carroll DM, Abriola LM. Influence of textural and wettability variations on predictions of DNAPL persistence and plume development in saturated porous media. Adv Water Resour 2004;27:411–27.
[32] Pulskamp K, Diabeté S, Krug HF. Carbon nanotubes show no sign of acute toxicity but induce intracellular reactive oxygen species in dependance on contaminants. Toxicol Lett 2007;168:58–74.
[33] Ramsburg CA, Abriola LM, Pennell KD, Loffler FE, Gamache M, Amos BK, et al. Stimulated microbial reductive dechlorination following surfactant treatment at the Bachman Road Site. Environ Sci Technol 2004;38(22):5902–14.
[34] Rehmann LLC, Welty C, Harvey RW. Stochastic analysis of virus transport in aquifers. Water Resour Res 1999;35(7):1987–2006.
[35] Saleh NB, Pfefferle LD, Elimelech M. Aggregation kinetics of multiwalled carbon nanotubes in aquatic systems: measurements and environmental implications. Environ Sci Technol 2008;42(21):7963–9.
[36] Scheibe TD, Dong HL, Xie YL. Correlation between bacterial attachment rate coefficients and hydraulic conductivity and its effect on field-scale bacterial transport. Adv Water Resour 2007;30(6–7):1571–82.
[37] Schwartz FW, Zhang H. Groundwater. 1st ed. New York: John Wiley & Sons Inc.; 2003.
[38] Sleep BE, Sykes JF. Compositional simulation of groundwater contamination by organic-compounds. 1. Model development and verification. Water Resour Res 1993;29(6):1697–708.
[39] Smith B, Wepasnick K, Schrote KE, Bertele AH, Ball WP, O'Melia C, et al. Colloidal properties of aqueous suspensions of acid-treated, multi-walled carbon nanotubes. Environ Sci Technol 2009;43(3):819–25.
[40] Stern ST, McNeil SE. Nanotechnology safety concerns revisited. Toxicol Sci 2008;101(1):4–21.
[41] Sun N, Elimelech M, Sun N-Z, Ryan JN. A novel two-dimensional model for colloid transport in a physically and geochemically heterogeneous porous media. J Contam Hydrol 2001;49:173–99.
[42] Tong Z, Bischoff M, Nies L, Applegate B, Turco RF. Impact of fullerence (C60) on a soil microbial community. Environ Sci Technol 2007;41(8):2985–91.
[43] Torkzaban S, Tazehkand SS, Walker SL, Bradford SA. Transport and fate of bacteria in porous media: coupled effects of chemical conditions and pore space geometry. Water Resour Res 2008;44:W04403. doi:04410.01029/02007WR006541.
[44] Tufenkji N, Redman JA, Elimelech M. Interpreting deposition patterns of microbial particles in laboratory-scale column experiments. Environ Sci Technol 2003;37(3):616–23.
[45] Tufenkji N, Miller GF, Ryan JN, Harvey RW, Elimelech M. Transport of cryptosporidium oocysts in porous media: role of straining and physicochemical filtration. Environ Sci Technol 2004;38(22):5932–8.
[46] Tufenkji N, Elimelech M. Correlation equation for prediction of single-collector efficiency in physiochemical filtration in saturated porous media. Environ Sci Technol 2004;38(2):529–36.
[47] Tufenkji N, Elimelech M. Deviation from the classical colloid filtration theory in the presence of repulsive DLVO interactions. Langmuir 2004;20(25): 10818–28.
[48] Tufenkji N, Elimelech M. Breakdown of colloid filtration theory: role of the secondary energy minimum and surface charge heterogeneities. Langmuir 2005;21(3):841–52.
[49] Wang P, Shi QH, Liang HJ, Steuerman DW, Stucky GD, Keller AA. Enhanced environmental mobility of carbon nanotubes in the presence of humic acid and their removal from aqueous solution. Small 2008;4(12):2166–70.
[50] Wiesner MR, Lowry GV, Alvarez P, Dionysiou D, Biswas P. Assessing the risks of manufactured nanomaterials. Environ Sci Technol 2006;40(14):4336–45.
[51] Yao KM, Habibian MT, O'Melia CR. Water and wastewater filtration – concepts and applications. Environ Sci Technol 1971;5(11):1105–12.